

Electrochemical behavior of reinforcing steel for nuclear reactor containment buildings

Maryam Qasem¹, Yongsun Yi², Sara Al Hanaei², Pyungyeon Cho²

¹(Emirates Nuclear Energy Corporation, Abu Dhabi, United Arab Emirates)

²(Department of Nuclear Engineering, Khalifa University, Abu Dhabi, United Arab Emirates)

Abstract: Electrochemical behavior of carbon steel for nuclear reactor containment buildings was investigated using potentiodynamic, potentiostatic, and galvanostatic polarization techniques in $\text{Ca}(\text{OH})_2$ solutions with NaCl. From potentiodynamic and potentiostatic polarization tests, it was found that the occurrence of pitting on the carbon steel in the solutions was strongly dependent on the applied potential and chloride concentration. Metastable pitting that has usually been observed on stainless steels in chloride containing solutions was not observed on the carbon steel used in this study. Using galvanostatic polarization technique, the chloride threshold conditions of the carbon steel were evaluated. First, samples were pre-passivated in $\text{Ca}(\text{OH})_2$ solutions without NaCl for 2 days by immersion. Then, galvanostatic current of $5\mu\text{A}/\text{cm}^2$ was applied to the pre-passivated samples. The occurrence of depassivation was evaluated as a function of pH and NaCl concentrations of solutions. Being expressed in the form of $[\text{OH}] = A([\text{Cl}])^n$ between the concentrations of OH^- and Cl^- , the exponents, n , of the chloride threshold conditions determined from the galvanostatic and potentiodynamic techniques were 0.3 and 0.35, respectively.

Keywords - Concrete reinforcing steel, depassivation, chloride threshold concentration, polarization

I. Introduction

In terms of the protection and the safety of plant-operating personnel and the general public as well as the environment, it is essential to ensure the proper performance and function of structures in commercial nuclear power plants [1]. Especially, reactor containment buildings in nuclear power plants play a role as the final barrier to radioactive material release and provide structural support [2]. Therefore, their structural integrity is very important over the service lives of nuclear power plants. Various types of degradation in concrete structures have been reported. According to the operation experience of NPPs in the USA, the following mechanisms are identified as the primary degradation mechanisms of reactor containment buildings: aggressive chemical attack, alkali-aggregate reactions, leaching, corrosion of reinforcing and pre-stressing steels, and stress relaxation of pre-stressed steel [3]. Among the aging and degradation phenomena, corrosion of reinforcing steels has been known as the leading mechanism determining the service life of reactor containment buildings in nuclear power plants [4,5] as well as general concrete structures [6].

The corrosion of reinforcing steel is mainly caused by carbonation and chloride ion (Cl^-) ingress [7]. Owing to the high alkalinity of the concrete pore water (pH over 12.5), a passive film is formed on reinforcing steels, which protects steels against corrosion attack [8]. When the pH of the pore solution is decreased by carbonation causing by penetrating carbon dioxide [9] or the chloride concentration on a steel surface embedded in concrete reaches its threshold condition [10], depassivation takes place on the surface, resulting in corrosion of reinforcing steels. Considering chloride ingress as a common cause of reinforced concrete structure degradation, numerous research efforts have been made on chloride ingress into concrete structures and its effect on depassivation and corrosion of reinforcing steels. The chloride transport through concrete occurs by four fundamental modes of chloride ions transportation through concrete: diffusion, capillary absorption, evaporative transport and hydrostatic [11] among which diffusion has been identified as the dominant transport mechanism [12]. Depassivation of reinforcing steels by chloride ions is governed by two parameters that are the diffusion coefficient of chloride ion through concrete and its threshold concentration at the surface of reinforcing steels. The diffusion coefficient of chloride in concrete depends on the concrete materials properties and environmental conditions [11,13]. Besides those material and environmental factors, the chloride threshold concentration should be affected by the electrochemical properties of reinforcing steels.

In this study, the electrochemical properties of a reinforcing steel used for reactor containment buildings were investigated by potentiodynamic and potentiostatic polarization experiments in $\text{Ca}(\text{OH})_2$ solutions with different concentrations of NaCl. Also, the chloride threshold concentration for the steel was determined in $\text{Ca}(\text{OH})_2$ solutions with different pH conditions. Through the comparison with data reported in previous studies, the measured electrochemical properties and threshold condition of the steel are discussed.

II. Experiment

2.1 Materials and Testing Environment

In this study electrochemical properties of a carbon steel that have been used as a reinforcing steel innuclear reactor containment buildingswere investigated. The chemical composition of the carbon steel was analyzed by glow discharge spectroscopy (GDS), which is given in Table 1. Test samples of $13 \times 13 \times 3$ mm were cut from carbon steel rebar and cold-mounted in epoxy resin with a wire connection to be used as a working electrode in electrochemical measurements. To prevent crevice corrosion between metallic surface and epoxy resin, the gaps were covered by a masking tape, leaving an exposed surface area of ~ 1 cm². Sample surfaces were ground up to # 800 SiC papers and ultrasonically cleaned and dried for electrochemical measurements.

Saturated Ca(OH)₂ solution was used as a reference solution representing the initial concrete pore conditions. To simulate different degrees of carbonation and chloride ion ingress in concrete, pH values and NaCl concentrations of solutions were adjusted by changing the amount of added Ca(OH)₂ and NaCl. Then, the electrochemical behavior of the carbon steel was evaluated as a function of pH and NaCl concentrations of solutions. The pH values of solutions were measured after 5 min. from the insertion of a pH sensor into the solutions. The conventional three electrode cell (electrolyte volume = ~ 800 ml) with a graphite as the counter electrode and a saturated calomel electrode (SCE) as the reference electrode was used. All the measurements were made in naturally aerated solutions at $22 \pm 2^\circ\text{C}$.

Table 1 Chemical composition of carbon steel (wt %)

Type	C	Si	Mn	P	S	Cr	Ni	Mo	Cu	Fe
Carbon steel	0.32	0.20	0.78	0.039	0.027	0.13	0.12	0.07	0.44	Bal.

2.2 Electrochemical Experiments

2.2.1 Potentiodynamic (PD) and Potentiostatic (PS) Polarization

The potentiodynamic polarization measurements on the steel were performed in Ca(OH)₂ solutions of two pH values of 11.7 and 12.4 (± 0.1). In Ca(OH)₂ solutions with different concentrations of NaCl, potentiodynamic polarization curves were measured using a potentiostat (Gamry Reference 3000) and analyzed as a function of Cl⁻ concentration. During 10 min. immersion of samples in test solutions, the open circuit potential (E_{ocp}) was measured, which was around -350 mV (vs. SCE). Before potentiodynamic scans, to reduce air-formed surface oxide, cathodic pre-treatment was performed by applying a cathodic potential of -850 mV (vs. SCE) to samples for 5 min. Then, from the pre-treatment potential samples of -850 mV (vs. SCE), samples were potentiodynamically polarized to the positive direction at a scan rate of 1 mV/s. Tests were stopped when the current density reached 5 mA·cm⁻². Potentiostatic polarization was performed in a saturated Ca(OH)₂ solution (pH = 12.4) with 0.4 M NaCl solution. After the cathodic pre-treatment at -850 mV (vs. SCE), different constant potentials from -300 to $+100$ mV (vs. SCE) between the corrosion potential and breakdown potential were applied to samples.

2.2.2 Galvanostatic (GS) Polarization

First, to form stable film on sample surfaces, a pre-passivation treatment was applied to samples by immersing them in saturated Ca(OH)₂ solution for two days. Krolkowski et al. [14] reported that at least two days would be required for a good surface passive state on carbon steels in alkaline solutions. The galvanostatic polarization was performed in Ca(OH)₂ solutions of which pH and NaCl concentration ranged from 10.5 to 12.4 and from 0.0002 to 0.4 M, respectively. The occurrence of depassivation on samples was identified as a potential drop from the oxygen evolution potential (OCP). The galvanostatic polarization consisted of two steps. In the first step, a constant current density of 5 $\mu\text{A}/\text{cm}^2$ was applied to samples for 30 min., which is designated by 1st GS. In the first step, depending on pH values and NaCl concentrations of test solutions, some samples showed potential drops indicating depassivation and others did not. If the potential did not drop over the time interval of the 1st GS step, a cathodic potential of -850 mV (vs. SCE) was potentiostatically applied for 5 min. This potentiostatic polarization was expected to induce an artificial damage to the surface film that was pre-formed in saturated Ca(OH)₂ solution. Then, as the second step the galvanostatic current was again applied to the samples for 30 min. (2nd GS) and the potentials were recorded. Tests were stopped when potential drops were observed. After galvanostatic polarization measurements, sample surfaces were examined by an optical microscope (OM) to confirm the occurrence of depassivation.

III. Results And Discussion

3.1 Potentiodynamic and Potentiostatic Polarization

Fig. 1 shows examples of potentiodynamic polarization curves of the carbon steel in Ca(OH)₂ solutions of pH 11.7 with and without NaCl. First, in Ca(OH)₂ solution of pH 11.7 without NaCl, the steel showed passivity soon right after the corrosion potential without an active current density peak in the anodic polarization, followed by a rapid increase in the current density at ~700 mV (vs. SCE). This potential corresponds to the oxygen evolution potential at pH 11.7 of which reaction is expressed by:



When NaCl of 0.001 M or lower concentration was added to Ca(OH)₂ solution, the corrosion potential decreased slightly with chloride concentration. The rapid increase in the current density was observed at the same potential as in the Ca(OH)₂ solution without NaCl addition. When chloride ions exist, the following reactions occur and they destroy the protective surface layers on reinforcing steels [8]:

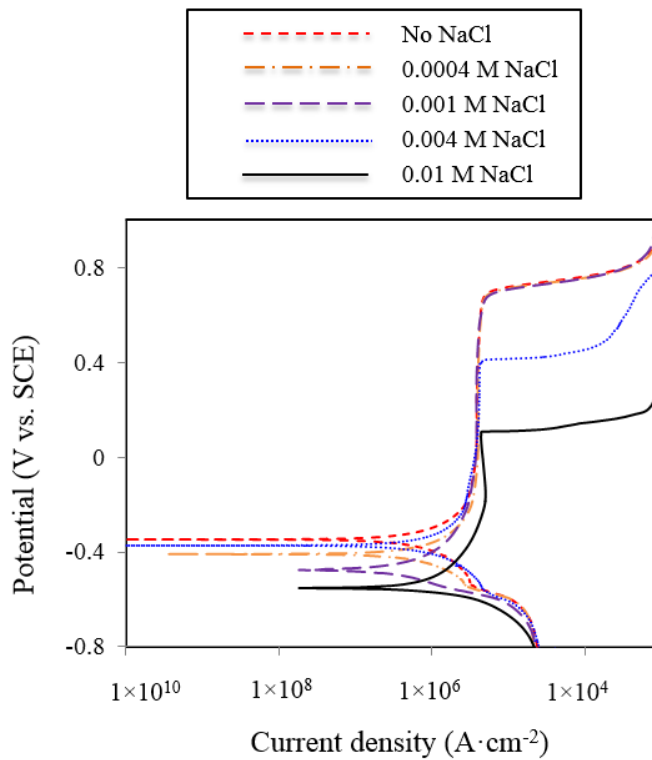
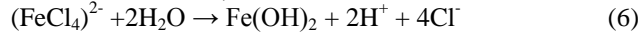
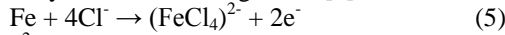


Fig.1. Potentiodynamic polarization curves of the carbon steel in Ca(OH)₂ solutions of pH 11.7 with different concentrations of NaCl.

The depassivation of metal surface causes localized corrosion, which is identified by a rapid increase in the current density. The measured breakdown potentials of the carbon steel in Ca(OH)₂ solution of pH 11.7 are summarized in Fig. 2. No pitting potentials were observed in the solutions containing NaCl smaller than 0.004 M. In Ca(OH)₂ solutions with 0.004 and 0.01 M NaCl, the pitting potentials were observed below the oxygen evolution potential, showing a decreasing trend with the Cl concentration.

This chloride concentration dependence of potentiodynamic polarization behavior has been well known and reported for carbon steels [16,17] and stainless steels [18]. Pistorius and Burstein [19] explain the chloride concentration dependence of the pitting potential in terms of the number of available sites for pitting. When the Cl⁻ concentration is reduced, there will be fewer sites available or slower reaction rates. According to the pit model by Galvele [20], a certain level of salt concentration is necessary to maintain the critical concentration of cations for pitting. Also, using the point defect model, Macdonald et al. [16,21] have developed another theoretical model explaining the chloride concentration dependence of the pitting potential. The exact mechanism of pitting on metals seems to be unclear yet. But, it is evident that there must exist a minimum chloride concentration for pitting of metals [22].

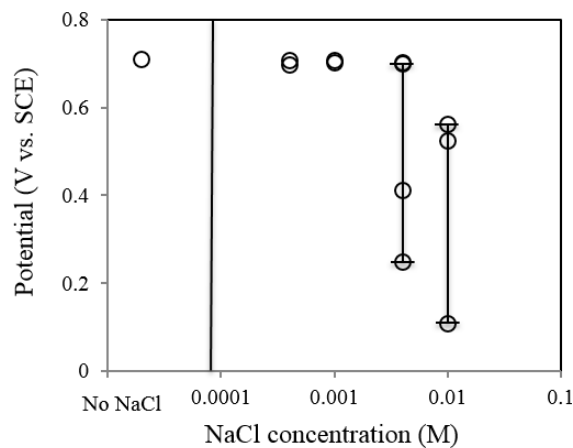


Fig. 2. Breakdown potentials of the steel as a function of the concentration of NaCl in $\text{Ca}(\text{OH})_2$ solutions of pH 11.7.

Fig. 2 shows that the pitting potentials of the carbon steel are widely scattered at high concentrations of NaCl while almost no data scatter appears on the oxygen evolution potential in solutions without NaCl or at relatively low concentrations of NaCl. This data scatter in pitting potential is considered to be due to less homogeneous surface film on carbon steel than stainless steels, which requires multiple measurements of pitting potential. The surface morphologies of the carbon steel after the potentiodynamic polarization measurements are compared in Figures 3 and 4. Optical micrographs of a sample potentiodynamically polarized up to different potentials in $\text{Ca}(\text{OH})_2$ solution of pH 11.7 with 0.0004 M NaCl are shown in Fig. 3. When the potentiodynamic polarization was stopped at 600 mV (vs. SCE) that is just before the oxygen evolution potential, a very clean surface was observed [Fig. 3(a)].

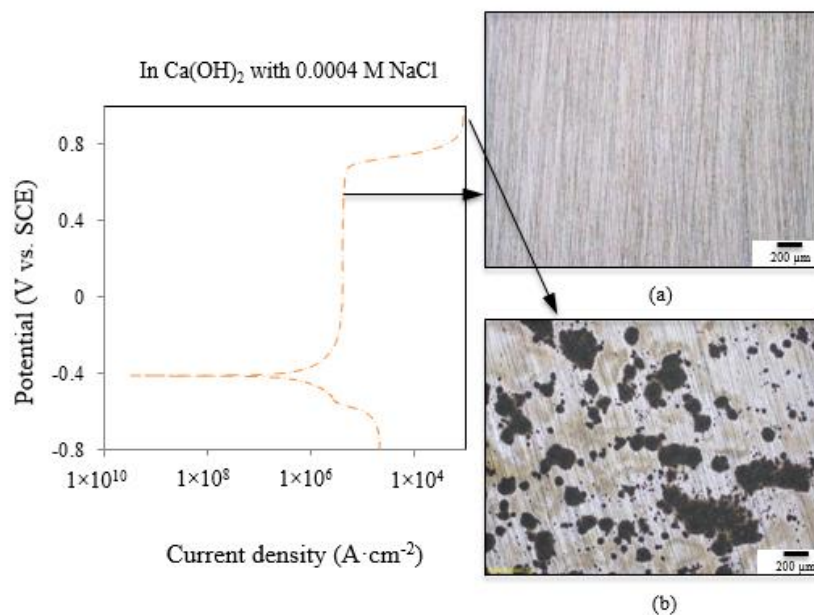


Fig. 3. Optical micrographs after the potentiodynamic polarization in $\text{Ca}(\text{OH})_2$ solution of pH = 11.7 with 0.0004 M NaCl (a) stopped at 600 mV (vs. SCE) and (b) passed the oxygen evolution potential.

Fig. 3(b) is an optical micrograph of the sample surface stopped when the current density reached $5 \text{ mA}\cdot\text{cm}^{-2}$ in $\text{Ca}(\text{OH})_2$ solution of pH 11.7 with 0.0004 M NaCl, showing corroded islands on the surface. This surface observation in Fig. 3 confirms that, in the solution with 0.0004 M NaCl, no depassivation occurred and consequently the current density had not undergone a rapid increase until the oxygen evolution potential on the polarization curve. On the other hand, the surface of the sample polarized in $\text{Ca}(\text{OH})_2 + 0.01 \text{ M NaCl}$, showed a severely corroded morphology over a wide range of an area (Fig. 4), which corresponds to the rapid increase in the current density at potentials far below than the oxygen evolution potential.

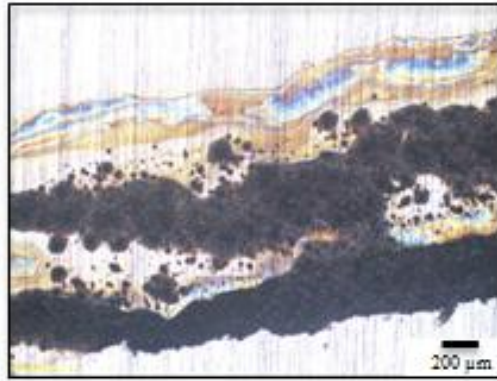


Fig. 4. Optical micrograph after the potentiodynamic polarization in Ca(OH)_2 solution with 0.01 M NaCl.

The effect of chloride concentration on the corrosion current densities, I_{corr} , of the steel in Ca(OH)_2 solutions was investigated. To determine the values of I_{corr} the four-point method developed by Jankowski and Juchniewicz [23] was used:

$$I = I_{corr} \left\{ \exp\left(\frac{\Delta E}{\beta_a}\right) - \exp\left(\frac{-\Delta E}{\beta_c}\right) \right\} \quad (7)$$

where ΔE is a potential range and β_a and β_c are Tafel constants of anodic and cathodic polarization, respectively. In this method, it is assumed that the polarization curves follow the Tafel behavior within a small potential range, ΔE , around the corrosion potential, E_{corr} . The potential intervals, ΔE , of 8 or 10 mV were used to calculate the corrosion current densities, which assumes that the logarithmic current densities have a linear relationship with the applied potential in the potential ranges. Fig. 5 shows the corrosion current densities, I_{corr} , of the carbon steel calculated on the potentiodynamic polarization curves in Ca(OH)_2 solutions with NaCl from 0 to 0.01M. The corrosion current densities were determined to range from $0.1 \sim 1 \mu\text{A}\cdot\text{cm}^{-2}$. It should be noted that almost no dependence on the NaCl concentration is observed in Fig. 5. It has been considered that chloride ions may be incorporated into surface films formed during potentiodynamic polarization. However, no dependence of I_{corr} on the concentration of chloride ions in the solutions implies that the added chloride ions to the solutions do not affect the electrochemical behavior of the steel until the applied potential reaches a certain potential during the potentiodynamic polarization causing pitting.

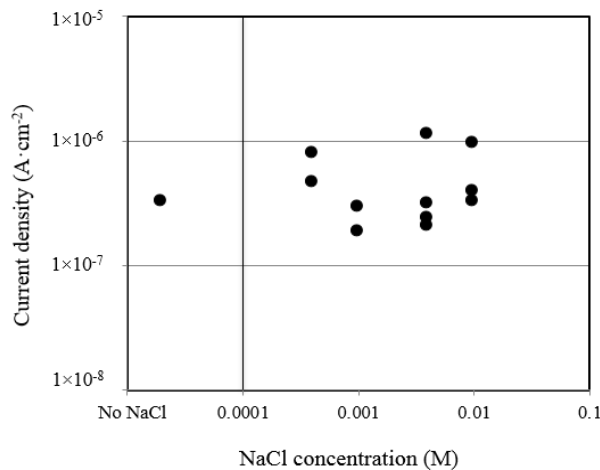


Fig. 5. Corrosion current densities during potentiodynamic polarization as a function of the concentration of NaCl.

The potentiostatic polarization curves of the carbon steel measured in saturated Ca(OH)_2 solutions (pH = 12.4) with 0.4 M NaCl are shown in Fig. 6. The applied potential dependence of the potentiostatic curves is clearly observed. At the potentials of -300 and -250 mV (vs. SCE) which are close to the corrosion potential, the current density decreases monotonically without any sign of depassivation. At -200 and -100 mV (vs. SCE) the current density first decreases and then increases quickly, indicating that depassivation took place by chloride ions. At 100 mV no decrease in the current density was observed, showing that corrosion occurred without passivation. Since the potential was applied right after the cathodic pretreatment, it is assumed that almost no

surface film exists on the sample surfaces. This current density behavior suggests that, at enough high potentials, chloride ions prohibit the formation of any surface hydroxide or oxide.

Another important observation from the potentiodynamic and potentiostatic polarization measurements is that no signs of metastable pit growth on the polarization curves were observed in Figs. 2 and 6. On potentiodynamic polarization curves of stainless steels in Cl containing solutions, metastable pit growth is identified as current density spikes [24,25]. Also, metastable pitting has been reported on carbon steels polarized potentiodynamically [16], potentiostatically [26], and in immersion tests [27]. In our previous work on stainless steels, metastable pitting has been clearly identified by current density spikes before stable pitting [25,28]. To detect metastable pitting, the current density data were collected at 10 Hz sampling rate (10 readings per sec.) during the polarization measurements. However, the polarization curve measured in pH 11.7 solution with 0.01 M NaCl (Fig. 2) showed a clean passive behavior without any current density spikes before the stable pitting indicated by the rapid increase in the current density. In Fig. 6(b), there was some data fluctuation before the increase in the current density. The metastable pitting is characterized by a slow current rise and rapid drop by repassivation [29]. The small current density fluctuation shown in Fig. 6(b) is quite different from the current density spikes indicating metastable pitting. Based on these observations it is concluded that during the potentiodynamic and potentiostatic polarization conditions, once the depassivation on the carbon steel occurs by Cl ions, the steel surface cannot be repassivated. This could be a property of the carbon steel used in this study that depends on the chemical composition and microstructures of the steel.

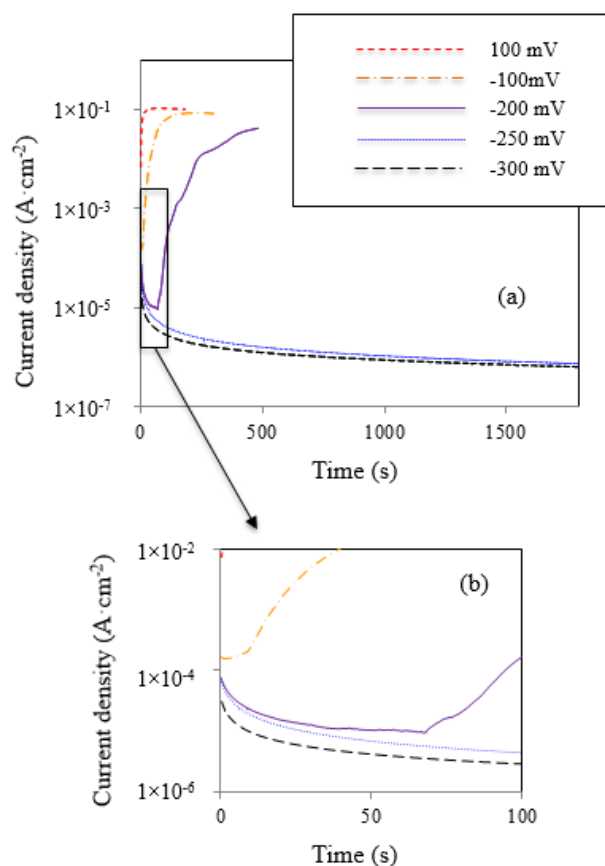


Fig. 6. Potentiostatic polarization curves of the steel determined at different potentials in saturated $\text{Ca}(\text{OH})_2$ solutions ($\text{pH} = 12.4$) with 0.4 M NaCl.

3.2 Galvanostatic Polarization

The results from the galvanostatic polarization measurements can be divided into three groups: i) potential drops in the 1stGS; ii) potential drops in the 2ndGS; iii) no potential drops over the entire test period. Fig. 7 shows an example of galvanostatic polarization results where a potential drop was observed during the 2nd GS mode. After the galvanostatic current was applied, the potential of samples increased rapidly to the oxygen evolution potential. Then, depending on the pH and concentrations of NaCl in $\text{Ca}(\text{OH})_2$ solutions, the potential was kept at the oxygen evolution potential or dropped to -300 ~ -400 mV (vs. SCE). When chloride ions exist in the solutions, the adsorption of the chloride ions on the metal surface film is facilitated by the positive potential

[29]. When chloride ions are sufficient to make the breakdown rate of the film higher than the film formation rate, depassivation occurs. This is observed on the galvanostatic curves as the potential drops, indicating the film breakdown by the aggressive ions in the solutions [30].

Fig. 8 shows the optical micrographs taken at different stages of the sample preparation and galvanostatic polarization measurements. Compared to the clean surface right after the mechanical grinding by SiC papers in Fig. 8(a), the sample surface after the 2 day immersion in saturated $\text{Ca}(\text{OH})_2$ solution showed corroded appearance with some back spots in Fig. 8(b). Fig. 8(c) shows an OM image of a sample undergoing the potential drop during the GS mode. A relatively large pit is observed in the figure, proving that the potential drops during the GS modes are due to the depassivation and pit occurrence on sample surfaces.

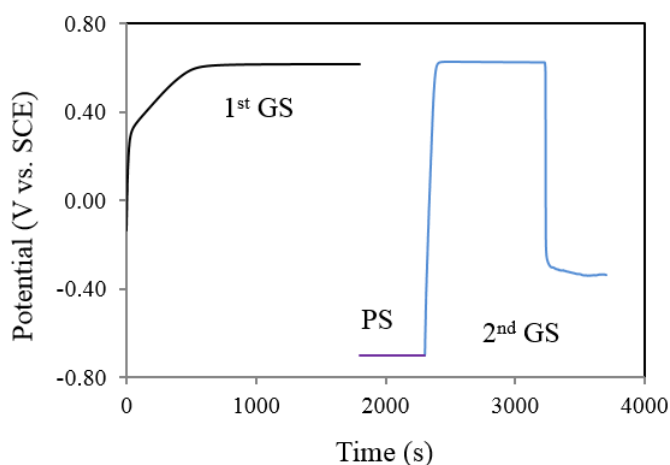


Fig. 7. An example of galvanostatic polarization behavior in saturated $\text{Ca}(\text{OH})_2$ with 0.1 M NaCl.

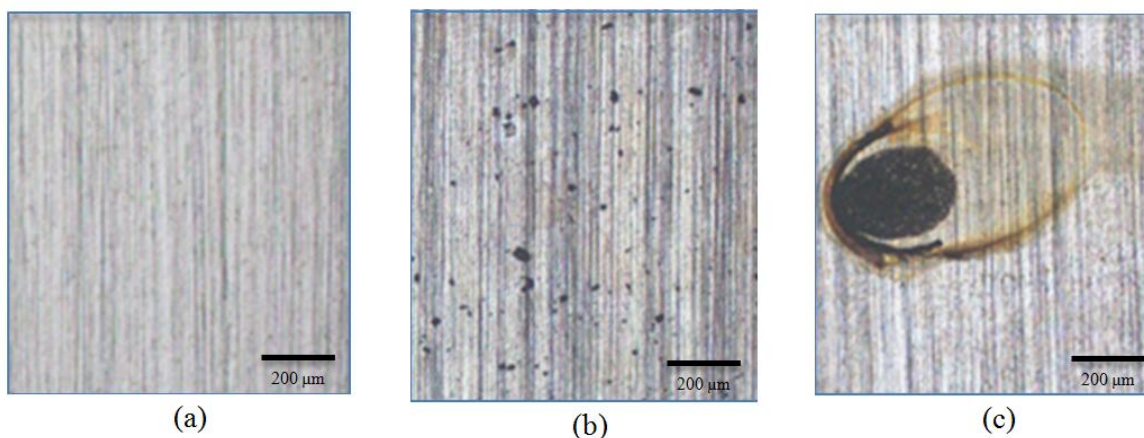


Fig. 8. Optical micrographs: (a) after mechanical grinding; (b) after the 2-day immersion in saturated $\text{Ca}(\text{OH})_2$ solution; (c) after the potential drop during GS mode.

The galvanostatic polarization measurement results are summarized in Fig. 9. The chloride ion concentration causing corrosion (depassivation) indicated by the potential drops during the galvanostatic polarization increases with pH, which is consistent with previous reports [31,32]. To induce damage to samples surface artificially, the potentiostatic polarization (PS) at a cathodic potential was applied to samples that had not shown potential drops in the 1st GS. The conditions in which potential drops were observed in the 2nd GS are plotted with a triangle symbol in Fig. 9. The degree of surface damage by the potentiostatic treatment was not quantitatively characterized. But, it is clearly shown that the potential drops of samples damaged by the PS treatment appeared at chloride ion concentrations lower than the 1st GS at a given pH value. This suggests that the initial state of the surface oxide is an important parameter in determining the chloride threshold concentration for depassivation of steels. Moreno et al. [33] compared the chloride threshold concentrations expressed as a mole concentration of NaCl from other publications. The chloride threshold concentrations from the literature are shown in Fig. 9 along with the data from this study. This comparison in Fig. 9 says that the pH dependence of the chloride threshold concentration determined in this study is in agreement with literature data.

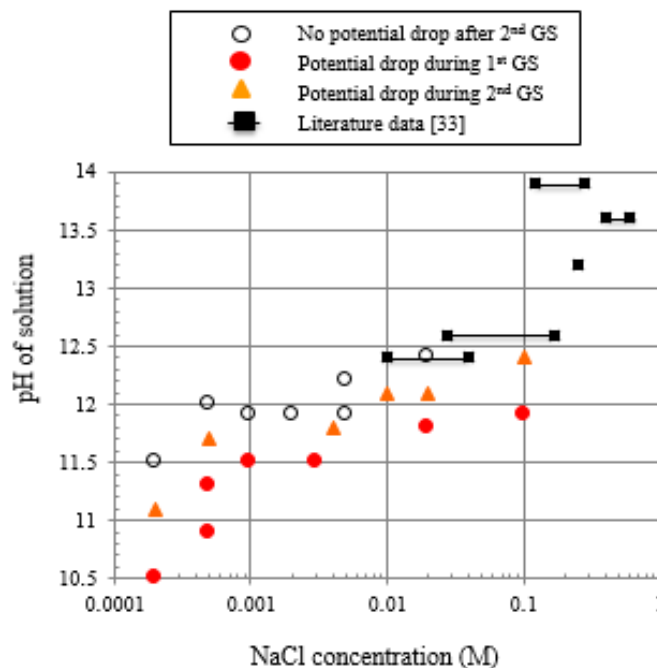


Figure 9: Dependence of depassivation of the carbon steel on pH and Cl concentration of solutions. Results are compared with literature data [33].

3.3 Chloride Threshold Concentration

The occurrence of depassivation of the carbon steel in $\text{Ca}(\text{OH})_2$ solutions with different pH values determined from the galvanostatic and potentiodynamic polarization techniques is shown in Fig. 10 as a function of chloride concentration. Gouda [34] proposed a linear relationship between pH and logarithmic values of the chloride threshold concentration for a pH range from 11.5 to 13.5:

$$pH = n \log([Cl]) + K \quad (8)$$

As shown in Fig. 10, the proportional constant, n , in the linear relationship was determined using straight lines following the smallest chloride concentrations that have caused depassivation at different pH values. The n values from the galvanostatic and potentiodynamic polarization are 0.30 and 0.35, respectively. The pH dependence of the chloride threshold concentration has been well recognized by a number of studies, which can be expressed in another form of equation 8:

$$[OH] = A [Cl]^n \quad (9)$$

where A is a constant and $[OH]$ and $[Cl]$ are concentrations of hydroxyl and chloride ions, respectively. The chloride threshold concentration has been expressed by total chloride contents, free chloride contents, a concentration ratio of chloride to hydroxyl ions [32,35,36]. Among the different expressions, $[Cl]/[OH]$ has been widely used. Adopting a probability model, Hausmann [37] proposed a constant value of $[Cl]/[OH]$, which corresponds to $n = 1$ in equation 8. This constant concentration ratio of chloride to hydroxyl ions has been used by some other researchers [38-40]. On the other hand, Gouda [34] reported 0.83 for the n value, which means that the ratio of $[Cl]/[OH]$ increases with pH values. Also, Li et al. [41] reported lower n values than 1. This is interpreted by a stronger inhibiting effect of the hydroxyl ions at higher pH conditions [32]. The n value determined in this study is smaller than those reported by other researchers previously. It is considered that the exponent, n , in equation 9 may be dependent on the electrochemical properties of reinforcing steels, which should be investigated as future study.

In Fig. 10, it is worth noting that the values of n determined from different methods, GS and PD, are close each other. In the galvanostatic tests, the surface films were formed in chloride free solutions and galvanostatic current density was applied to the films in chloride containing solutions. In this condition, during the galvanostatic polarization, chloride ions should be adsorbed and penetrate through chloride free surface films to cause depassivation. On the other hand, in the potentiodynamic polarization, from the early stage of film formation chloride ions are incorporated into surface films. Despite different conditions of surface film formation between the GS and PD experiments, the n values were determined close each other. These results suggest that the potentiodynamic polarization may be used to determine the threshold chloride conditions as a quick and simple method.

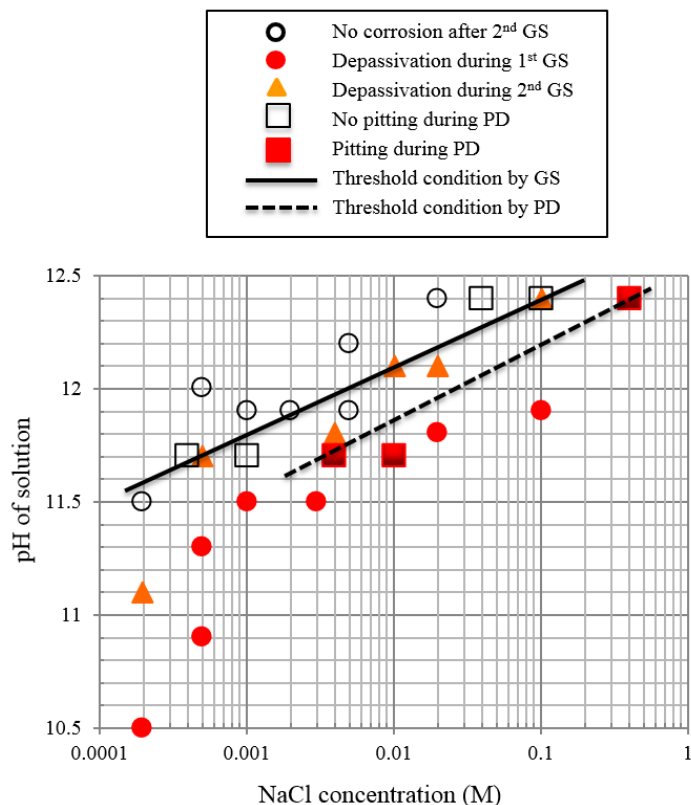


Fig. 10. Threshold conditions for the depassivation of the carbon steel determined by the galvanostatic and potentiodynamic polarization.

IV. Conclusions

The electrochemical behavior and chloride threshold concentrations for a carbon steel from nuclear power plants were evaluated in $\text{Ca}(\text{OH})_2$ solutions using galvanostatic, potentiodynamic, and potentiostatic polarization experiments. The following conclusions can be drawn:

- During the potentiodynamic polarization, depassivation and pitting on the carbon steel occurred at chloride concentrations higher than certain levels that depends on pH of the solutions.
- The applied potential dependency of the current densities in potentiostatic polarization was similar to that well known for stainless steels in Cl^- containing solutions.
- During potentiodynamic and potentiostatic polarization, no current density spikes as a sign of metastable pitting were observed, suggesting that surface on this steel cannot be repassivated once the depassivation occurs by chloride ions.
- The addition of NaCl to the test solution did not affect the corrosion current densities, I_{corr} , determined from the potentiodynamic polarization curves. In potentiostatic polarization, at low applied potentials, monotonic decrease in the current densities was observed.
- In terms of the threshold conditions, a linear relationship between logarithmic values of $[\text{OH}^-]$ and $[\text{Cl}^-]$. Expressed in the form of $[\text{OH}^-] = A([\text{Cl}^-])^n$, the exponent, n , was determined 0.3 and 0.35 from the galvanostatic and potentiodynamic techniques, respectively.
- The potentiodynamic polarization gave rise to the threshold chloride contents comparable to those from the galvanostatic and literature data, which suggests that the potentiodynamic polarization technique may be used for the purpose as a quick and simple method.

Acknowledgements

The authors are grateful for the financial support and test facilities provided by Khalifa University and the support from Emirates Nuclear Energy Corporation (ENEC) for Maryam Qasem and Sara Al Hanaei. The preliminary results of this study were presented at EUROCORR 2015 in September 6-10, 2015 in Graz, Austria.

References

- [1] D.J. Naus, Concrete, Comprehensive Nuclear Materials, 4, 2012, 407-431.
- [2] M.J. Do, A.D. Chockie, Aging degradation of concrete structures in nuclear power plants, SKI Report 94:15, Sept. 1994.

- [3] V.N. Shah, C.J. Hookham, Long-term aging of light water reactor concrete containments, *Nuclear Engineering and Design*, 185, 1998, 51-81.
- [4] IAEA, Assessment and management of major nuclear power plant components important to safety, IAEA-TECDOC-1025, 1998.
- [5] B.R. Ellingwood, Y. Mori, Probabilistic methods for condition assessment and life prediction of concrete structures in nuclear power plants, *Nuclear Engineering and Design*, 142, 1993, 155-166.
- [6] L. Yu, R. François, V.H. Dang, V. L'Hostis, R. Gagné, Distribution of corrosion and pitting factor of steel in corroded RC beams, *Construction and Building Materials*, 95, 2015, 384-392.
- [7] C.L. Page, K.W.J. Treadaway, Aspects of the electrochemistry of steel in concrete, *Nature*, 297, 1982, 109-115.
- [8] B.N. Popov, Corrosion of structural concrete, *Corrosion Engineering*, 2015, 525-556.
- [9] A. Steffens, D. Dinkler, H. Ahrens, Modelling carbonation for corrosion risk prediction of concrete structures, *Cement and Concrete Research*, 32, 2002, 935-941.
- [10] C.A. Apostolopoulos, S. Demis, V.G. Papadakis, Chloride-induced corrosion of steel reinforcement – Mechanical performance and pit depth analysis, *Construction and Building Materials*, 388, 2013, 139-146.
- [11] E. Badogiannis, E. Aggeli, V.G. Papadakis, S. Tsivilis, Evaluation of chloride-penetration resistance of metakaolin concrete by means of a diffusion - Binding model and of the k-value concept, *Cement and Concrete Research*, 63, 2015, 1-7.
- [12] S.M. Samadi, M.K. Samarakoon, J. Sælensminde, Condition assessment of reinforced concrete structures subject to chloride ingress: A case study of updating the model prediction considering inspection data, *Cement and Concrete Research*, 60, 2015, 92-98.
- [13] K.A.T. Vu, M.G. Stewart, Structural reliability of concrete bridges including improved chloride-induced corrosion models, *Structural Safety*, 22, 2000, 313-333.
- [14] A. Królikowski, J. Kuziak, Impedance study on calcium nitrite as a penetrating corrosion inhibitor for steel in concrete, *Electrochimica Acta*, 56, 2011, 7845-7853.
- [15] G.S. Frankel, Pitting corrosion of metals – A review of the critical factors, *Journal of the Electrochemical Society*, 145(6), 1998, 2186-2198.
- [16] S. Sharifi-Asl, F. Mao, P. Lu, B. Kursten, D.D. Macdonald, Exploration of the effect of chloride ion concentration and temperature on pitting corrosion of carbon steel in saturated Ca(OH)₂ solution, *Corrosion Science*, 98, 2015, 708-715.
- [17] L. Bertolini, E. Redaelli, Depassivation of steel reinforcement in case of pitting corrosion: detection techniques for laboratory studies, *Materials and Corrosion*, 60(8), 2009, 608-616.
- [18] N.J. Laycock, R.C. Newman, Localized dissolution kinetics, salt films and pitting potentials, *Corrosion Science*, 39, 1997, 1771-1790.
- [19] P.C. Pistorius, G.T. Burstein, Aspects of the effects of electrolyte composition in the occurrence of metastable pitting on stainless steel, *Corrosion Science*, 36(3), 1994, 525-538.
- [20] J.R. Galvele, Transport processes and the mechanism of pitting of metals, *Journal of the Electrochemical Society*, 123(4), 1976, 464-474.
- [21] L.F. Lin, C.Y. Chao, D.D. Macdonald, A Point defect model for anodic passive films – II. Chemical breakdown and pit initiation, *Journal of the Electrochemical Society*, 128(6), 1981, 1194-1198.
- [22] T. Hong, M. Nagumo, The effect of chloride concentration on early stages of pitting for Type 304 stainless steel revealed by the AC impedance method, *Corrosion Science*, 39(2), 1997, 285-293.
- [23] J. Jankowski, R. Juchniewicz, A four-point method for corrosion rate determination, *Corrosion Science*, 20, 1980, 841-851.
- [24] G.T. Burstein, P.C. Pistorius, S.P. Mattin, The nucleation and growth of corrosion pits on stainless steel, *Corrosion Science*, 35, 1993, 57-62.
- [25] M. Al Ameri, Y. Yi, P. Cho, S. Al Saadi, C. Jang, P. Beeley, Critical conditions for pit initiation and growth of austenitic stainless steels, *Corrosion Science*, 92, 2015, 209-216.
- [26] Y.F. Cheng, J.L. Luo, Metastable pitting of carbon steel under potentiostatic control, *Journal of the Electrochemical Society*, 146(3), 1999, 970-976.
- [27] Z.H. Dong, W. Shi, X.P. Guo, Initiation and repassivation of pitting corrosion of carbon steel in carbonated concrete pore solution, *Corrosion Science*, 53, 2011, 1322-1330.
- [28] Y. Yi, P. Cho, A. Al Zaabi, Y. Addad, C. Jang, Potentiodynamic polarization behavior of AISI type 316 stainless steel in NaCl solution, *Corrosion Science*, 74, 2013, 92-97.
- [29] K.S. Rajagopalan, K. Venu, K. Balakrishnon, Anodic polarization studies in neutral and alkaline solutions containing corrosion inhibitors, I. NaOH-NaCl system, *Journal of the Electrochemical Society*, 119(2), 1962, 81-87.
- [30] O. Poupard, A. Ait-Mokhtar, and P. Dumargue, Corrosion by chlorides in reinforced concrete: Determination of chloride concentration threshold by impedance spectroscopy, *Cement and Concrete Research*, 34, 2004, 991-1000.
- [31] K.Y. Ann, H-W. Song, Chloride threshold level for corrosion of steel in concrete, *Corrosion Science*, 49, 2007, 4113-4133.
- [32] U. Angst, B. Elsener, C. K. Larsen, Ø. Vennesland, Critical chloride content in reinforced concrete — A review, *Cement and Concrete Research*, 39, 2009, 1122-1138.
- [33] M. Moreno, W. Morris, M.G. Alvarez, G.S. Duffo, Corrosion of reinforcing steel in simulated concrete pore solutions - Effect of carbonation and chloride content, *Corrosion Science*, 46, 2004, 2681-2699.
- [34] V.K. Gouda, Corrosion and corrosion inhibition of reinforcing steel – I. Immersed in alkaline solutions, *British Corrosion Journal*, 5, 1970, 198-203.
- [35] G.K. Glass, N.R. Buenfeld, The presentation of the chloride threshold level for corrosion of steel in Concrete, *Corrosion Science*, 39(5), 1997, 1001-1013.
- [36] G.R. Meira, C. Andrade, E.O. Vilar, K.D. Nery, Analysis of chloride threshold from laboratory and field experiments in marine atmosphere zone, *Construction and Building Materials*, 55, 2014, 289-298.
- [37] D.A. Hausmann, Steel corrosion in concrete, *Materials Protection*, 6, 1967, 19-23.
- [38] S. Goni, C. Andrade, Synthetic concrete pore solution chemistry and rebar corrosion rate in the presence of chlorides, *Cement and Concrete Research*, 20, 1990, 525-539.
- [39] L. Jiang, G. Huang, J. Xu, Y. Zhu, L. Mo, Influence of chloride salt type on threshold level of reinforcement corrosion in simulated concrete pore solutions, *Construction and Building Materials*, 30, 2012, 516-521.
- [40] H. Nahali, L. Dhoubi, H. Idrissi, Effect of phosphate based inhibitor on the threshold chloride to initiate steel corrosion in saturated hydroxide solution, *Construction and Building Materials*, 50, 2014, 87-94.
- [41] L. Li, A.A. Sagues, Chloride corrosion threshold of reinforcing steel in alkaline solutions – open-circuit immersion tests, *Corrosion Science*, 57(1), 2001, 19-28.

